New Rotation Free Shell Triangle for Crash-Worthiness Analysis in Parallel PC Networks

E. Oñate
F. Zárate
X. Plana
L. Neamtu

Publication CIMNE Nº 168, July 1999

New Rotation Free Shell Triangle for Crash-Worthiness Analysis in Parallel PC Networks

E. Oñate
F. Zárate
X. Plana
L. Neamtu

Publication CIMNE Nº 168, July 1999

International Center for Numerical Methods in Engineering
Gran Capitán s/n, 08034 Barcelona, Spain

NEW ROTATION FREE SHELL TRIANGLE FOR CRASH-WORTHINESS ANALYSIS IN PARALLEL PC NETWORKS

E. Oñate[1], F. Zárate[1], X. Plana[2], L. Neamtu[2]

[1] *International Centre for Numerical Methods in Engineering*
Universidad Politécnica de Cataluña, 08034 Barcelona, Spain

[2] *Quantech ATZ, S.A., Edificio NEXUS*
Jordi Girona Salgado, s/n, 08034 Barcelona, Spain

ABSTRACT

A new three node shell triangular element with translational degree of freedom as the only modal variables is presented. The element formulation is based on combining a standard linear finite element interpolation with a cell centered finite volume scheme. Details of the implementation of the element in an explicit dynamic code operating in parallel on networks of PC's are presented. The efficiency and applicability of the new rotation free shell triangle is shown in the solution of some contact/impact and crash-worthiness problem.

1 INTRODUCTION

The need for efficient plate and shell elements is critical for solving large scale structural problems in industry such as the analysis of vehicle crash-worthiness situations. The derivation of simple triangles capable of accurately representing the shell deformation under complex loading conditions is still nowadays the objective of intensive research [1].

Several authors have tried to derive finite elements with displacements as the only nodal variables. So far the methods proposed limit their applicability to triangular element shapes only. Barnes [2] proposed a method for deriving a three node triangle with three nodal degrees of freedom (d.o.f.) based on the computation of the curvatures in terms of the normal rotations at the mid-side points determined from the nodal deflections of adjacent elements. This method has also been exploited by Hampshire *et al.* [3] assuming that the elements are hinged together at their common boundaries, the bending stiffness being represented by torsional springs resisting the rotations about the hinge lines. Phaal and Calladine [4,5] have proposed a similar class of triangles for plate and shell analysis. Yang *et al.* [6] derived a family of elements of this type based on the so-called bending energy augmented membrane approach which basically reproduces the hinge bending stiffness procedure of Hampshire *et al.* [3]. Brunet and Sabourin [7] proposed a different approach to compute the constant curvature field within each element in terms of the six node displacements of a macro-element. The element was successfully applied to nonlinear shell analysis using an explicit dynamic approach. More recently Rio *et al.* [8] have used the concept of side hinge bending stiffness to derive a thin shell triangle of "translational" kind for explicit dynamic analysis of sheet stamping problems.

Oñate and Cervera [9] have proposed a general procedure based on combining finite element (FE) and finite volume (FV) concepts [10,11] for deriving thin plate elements with translational degrees of freedom only and presented a competitive three d.o.f. plate triangle. This element has been successfully extended to shell analysis by Zárate (1996). The nine d.o.f. thin shell element has been further developed to deal with sheet forming problems using a non linear explicit dynamic program[14-16].

In this paper advances in the so called Basic Shell Triangle (BST) for analysis of contact/impact problems are described. The BST element combines a linear FE approximation with a cell centered FV scheme [10-11]. The content of the paper includes a brief description of the main ingredients of the formulation of the BST element and its implementation in a explicit dynamic code operating on parallel networks of PC's. Some examples of the efficiency of the new rotation free triangle for analysis of contact/impact and crash-worthiness problems are presented.

2 BASIC SHELL TRIANGLE (BST)

Figure 1 shows the patch of four shell triangles typical of the BST formulation. As usual in the cell centered finite volume scheme the control domain coincides with an individual element.

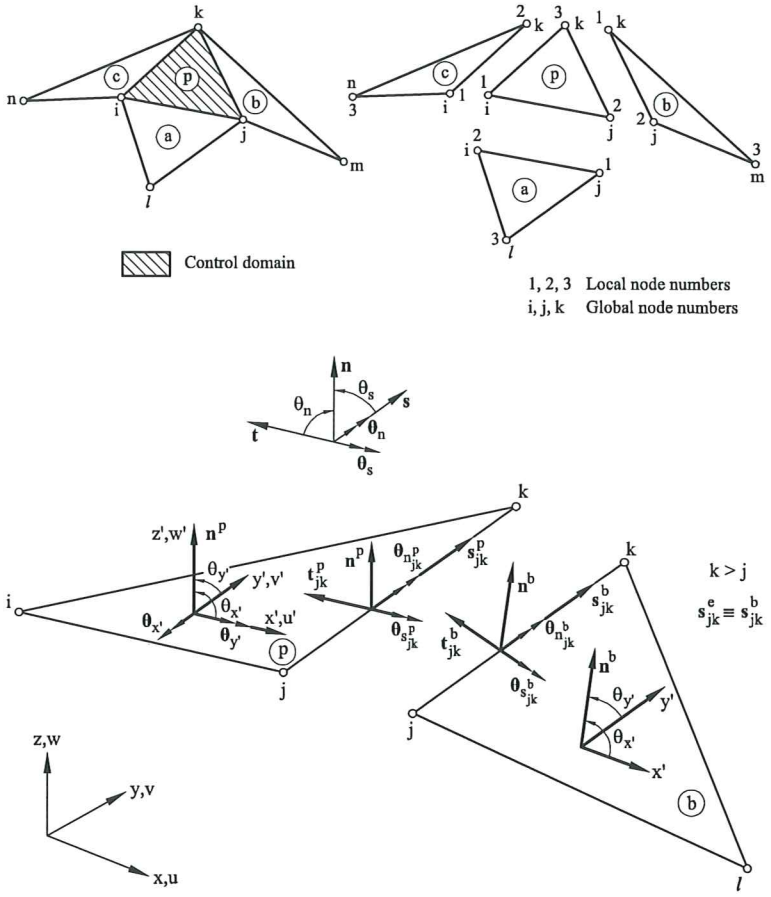

Figure 1. Basic shell triangle (BST)

For convenience let us express the local rotations $\theta_{x'}, \theta_{y'}$ along each side in terms of the tangential and normal side rotations θ_s and θ_n.

The transformation relating local and side rotations (Figure 1) is written as

$$\boldsymbol{\theta}'^{(e)} = \left\{ \begin{matrix} \theta_{x'} \\ \theta_{y'} \end{matrix} \right\}^{(e)} = \begin{bmatrix} c_{ij} & -s_{ij} \\ s_{ij} & c_{ij} \end{bmatrix}^{(e)} \left\{ \begin{matrix} \theta_{s_{ij}} \\ \theta_{n_{ij}} \end{matrix} \right\}^{(e)} = \hat{\mathbf{T}}_{ij} \hat{\boldsymbol{\theta}}'_{ij} \tag{1}$$

where $\theta_{s_{ij}}$ and $\theta_{n_{ij}}$ are the tangential and normal rotations along side ij of element e, $\theta_{x'} = \frac{\partial w'}{\partial x'}$, $\theta_{y'} = \frac{\partial w'}{\partial y'}$ and $c_{ij}^{(e)}$, $s_{ij}^{(e)}$ are the components of side vector $\mathbf{s}_{ij}^{(e)}$, i.e. $\mathbf{s}_{ij}^{(e)} = [c_{ij}^{(e)}, s_{ij}^{(e)}]^T$.

The local curvatures over the control domain formed by the triangle ijk is given by

$$\boldsymbol{\kappa}'_p = \int\int_{A^{(P)}} \boldsymbol{\kappa}' dA = \frac{1}{A^{(p)}} \int_{\Gamma_p} \mathbf{T} \boldsymbol{\nabla}' w' d\Gamma \tag{2}$$

where

$$\boldsymbol{\kappa}' = \left[-\frac{\partial^2 w'}{\partial x'^2}, -\frac{\partial^2 w'}{\partial y'^2}, -2\frac{\partial^2 w'}{\partial x' \partial y'} \right]^T \tag{3}$$

$$\mathbf{T} = \begin{bmatrix} -t_x & 0 & -t_y \\ 0 & -t_y & -t_x \end{bmatrix}^T \qquad \text{and} \quad \boldsymbol{\nabla}' = \begin{Bmatrix} \frac{\partial}{\partial x'} \\ \frac{\partial}{\partial y'} \end{Bmatrix}$$

where $t_{x'}$, $t_{y'}$ are the components of the vector $\mathbf{t}$ in the x', y' coordinate system. The transformation of the area integral of eq.(2) into a line integral is typical of finite volume methods [10,11].

Recalling that $\boldsymbol{\theta}' = [\theta_{x'}, \theta_{y'}]^T = \boldsymbol{\nabla}' w'$ and substituting the curvature over the triangular control domain can be written as

$$\boldsymbol{\kappa}'_p = \frac{1}{A^{(p)}} [\mathbf{T}^{(p)}_{ij} \hat{\mathbf{T}}^{(p)}_{ij} \hat{\boldsymbol{\theta}}'_{ij} l_{ij} + \mathbf{T}^{(p)}_{jk} \hat{\mathbf{T}}^{(p)}_{jk} \hat{\boldsymbol{\theta}}'_{jk} l_{jk} + \mathbf{T}^{(p)}_{ki} \hat{\mathbf{T}}^{(p)}_{ki} \hat{\boldsymbol{\theta}}'_{ki} l_{ki}] \tag{4}$$

In the derivation of eq. (4) it has been assumed that the local rotations are constant over each element side. This is a consequence of the linear interpolation chosen for the displacement field.

The tangential side rotations are expressed in terms of the local deflections along the sides. For instance, for side jk

$$\theta^{(p)}_{s_{jk}} = \frac{w'^{(p)}_k - w'^{(p)}_j}{l_{jk}} \quad \text{for } k > j \tag{5}$$

where l_{jk} is the length of side jk.

Equation (5) introduces an approximation as the tangential rotation vectors of adjacent elements sharing a side are not parallel. Therefore the tangential rotations are discontinuous along element sides. The authors have found that this discontinuity has little relevance in practice.

The normal rotation vector has the same direction for the two elements sharing a side (Figure 1). A *continuous* value of the normal rotation along the side can enforced by defining an average normal side rotation as

$$\theta^{(p)}_{n_{jk}} = \frac{1}{2}(\theta^{(p)}_{n_{jk}} + \theta^{(b)}_{n_{jk}}) = \frac{1}{2} \left(\boldsymbol{\lambda}^{(p)}_{jk} \boldsymbol{\nabla}' w'^{(p)} + \boldsymbol{\lambda}^{(b)}_{jk} \boldsymbol{\nabla}' w'^{(b)} \right) \tag{6}$$

where

$$\boldsymbol{\lambda}^{(p)}_{jk} = [-s^{(p)}_{jk}, c^{(p)}_{jk}] \tag{7}$$

Substituting eqs. (5) and (6) into (4) and choosing a standard linear interpolation for the deflection field within each triangle [18], the curvatures for the control domain can be expressed in term of the normal deflection values of patch nodes as

$$\boldsymbol{\kappa}'_p = \mathbf{S}_p \boldsymbol{w}'_p, \qquad \mathbf{S}_p = [\mathbf{S}^{(p)}_{ij}, \mathbf{S}^{(p)}_{jk}, \mathbf{S}^{(p)}_{ki}] \tag{8}$$

$$\boldsymbol{w}'_p = [w'^{(p)}_i, w'^{(p)}_j, w'^{(p)}_k, w'^{(a)}_j, w'^{(a)}_i, w'^{(a)}_l, w'^{(b)}_k, w'^{(b)}_j, w'^{(b)}_m, w'^{(c)}_i, w'^{(c)}_k, w'^{(c)}_n]^T \tag{9}$$

The form of the different $\mathbf{S}^{(p)}_{ij}$ matrices is given in [13]. Note also that the definition of vector $\boldsymbol{w}'_p$ depends on the convenion chosen for the local and global node numbers for the element patch.

The normal nodal deflections are related to the global nodal displacements by the following transformation

$$\boldsymbol{w}'_p = \mathbf{C}_p \mathbf{a}_p \tag{10}$$

Substituting eq. (10) into (8) gives finally

$$\boldsymbol{\kappa}'_p = \mathbf{B}_{b_p} \mathbf{a}_p \quad \text{with} \quad \mathbf{B}_{b_p} = \mathbf{S}_p \mathbf{C}_p \tag{11}$$

In above $\mathbf{a}_p$ is the vector containing the eighteen nodal displacement variables of the six nodes belonging to the patch of elements associated to the p-th control domain. Recall that in the BST element control domains coincide with triangles.

The bending stiffness matrix associated to the p-th control domain is obtained by

$$\mathbf{K}_{b_p} = A^{(p)} \mathbf{B}_{b_p}^T \mathbf{D}_b \mathbf{B}_{b_p} \tag{12}$$

where $\mathbf{D}_b$ is the bending constitutive matrix.

The membrane contribution to the BST element is simply provided by the Constant Strain Triangle (CST) under plane stress conditions [20].

The stiffness matrix for the BST element is obtained by adding the membrane and bending contributions, i.e.

$$\mathbf{K}_p = \mathbf{K}_{b_p} + \mathbf{K}_{m_p} \tag{13}$$

where $\mathbf{K}_{b_p}$ is given by eq. (12) and $\mathbf{K}_{m_p}$ is the membrane stiffness matrix for the CST element adequately extended to account for the degrees of freedom of the elements contributing to each control domain [13].

Recall that the dimensions of the stiffness matrix $\mathbf{K}_p$ is 18×18 as it links the eighteen displacements of the six nodes contributing to the control domain. The assembly of the stiffness matrices $\mathbf{K}_p$ into the global equation system follows the standard procedure, i.e. a control domain is treated as a macro-triangular element with six nodes.

The equivalent nodal force vector is obtained similarly as for standard C_0 shell triangular elements. Thus, the contribution of a uniformly distributed load over an element is splitted into three equal parts among the three element nodes. As usual nodal point loads are directly asigned to a node.

The procedure for prescribing the boundary conditions for the BST element is simplified as the side rotations are formulated in terms of the normal and tangential values. This allows to treat naturally all boundary condition types found in practice. Thus, the conditions on the normal rotations are introduced when forming the curvature matrix, whereas the conditions on the nodal displacements and the tangential rotations are prescribed at the equation level solution.

The BST element has been implemented within the commercial sheet stamping code SIMPACT [17]. Details of the parallel computing scheme SIMPACT are described in next sections. Further informations on the BST element can be found in [13].

3 PARALLEL EXPLICIT DYNAMIC ANALYSIS

The dynamic equilibrium equations are written in terms of the principle of virtual work using an updated Lagrangian formulation. The discretized form of equilibrium is obtained in the standard manner:

$$\mathbf{M}\ddot{\mathbf{a}} + \mathbf{C}\dot{\mathbf{a}} = \mathbf{f} - \mathbf{p} - \mathbf{f}_c \tag{14}$$

where $\mathbf{M}$ is the mass matrix, $\mathbf{C}$ the damping matrix, $\ddot{\mathbf{a}}$ the vector of nodal accelerations, $\dot{\mathbf{a}}$ the vector of nodal velocities, $\mathbf{f}$ the vector of external loading, $\mathbf{p}$ the vector of internal forces and $\mathbf{f}_c$ the vector of contact forces.

A diagonal mass matrix obtained by a lumping procedure applied to the element consistent mass matrices is used and the damping matrix is assumed to be of the form $\mathbf{C} = 2\alpha\mathbf{M}$, α being a damping parameter. The equations of motion are integrated by the central difference method and, using the assumption that the $\mathbf{M}$ and $\mathbf{C}$ matrices are diagonal, this gives rise to an explicit dynamic formulation for the BST element [16–18].

The numerical procedure used to integrate the equations of motion (14) from time step n to time step $n+1$ is as follows:

1. At time step n the vectors $\mathbf{a}^n, \dot{\mathbf{a}}^{n-1/2}, \mathbf{f}^n, \mathbf{p}^n, \mathbf{f}_c^n$ are known at the nodes and the strain and stress tensors, $\boldsymbol{\epsilon}^n$ and $\boldsymbol{\sigma}^n$ respectively, are known for each element.

2. Compute the accelerations at all nodes: $\ddot{\mathbf{a}}^n = \mathbf{M}_D^{-1}[\mathbf{f} - \mathbf{p} - \mathbf{f}_c - \mathbf{C}\dot{\mathbf{a}}]^n$, where $\mathbf{M}_D = \text{diag } \mathbf{M}$.

3. Compute velocities and displacements at all nodes:

$$\begin{aligned} \dot{\mathbf{a}}^{n+1/2} &= \dot{\mathbf{a}}^{n-1/2} + \ddot{\mathbf{a}}^n \Delta t^{n+1/2} \\ \mathbf{a}^{n+1} &= \mathbf{a}^n + \dot{\mathbf{a}}^{n+1/2} \Delta t^{n+1} \end{aligned}$$

   where $\Delta t^{n+1/2} = \frac{1}{2}[\Delta t^n + \Delta t^{n+1}]$.

4. Compute strains and stresses for all elements: $\boldsymbol{\epsilon}^{n+1}$, $\boldsymbol{\sigma}^{n+1}$.

5. Compute the internal force vector at all nodes and assemble: $\mathbf{p}^{n+1} = \mathbf{B}^T \boldsymbol{\sigma}^{n+1} A^{(e)}$.
   where $\mathbf{B}$ is the strain matrix accounting for bending and membrane effects.

6. Check for frictional contact conditions and compute the contact force vector $\mathbf{f}_c$.

7. Computer the external force vector $\mathbf{f}$.

8. Go to step 1 for the next time step.

Conditional stability of the explicit time integration requires that the time step size must not exceed a critical time step size $\Delta t_{\text{crit}}^{(e)} = \frac{2}{w_m}$, where w_m is the lowest period of vibration. Finding this value allows a critical time step size to be computed at each step (or at pre-determined intervals) which therefore provides an automatic time-stepping procedure.

The basic philosophy of the parallel computing scheme is that each processor carries out exactly the same function but on a different domain (there are no master-slave relationships). This is effectively a SPMD (Single Program Multiple Data) structure. To do this effectively and with as much transparency to the user as possible it is necessary to carry out the domain decomposition and analysis steps as automatically as possible. The following scheme is thus utilized:

- Create the geometry, assign the problem attributes and generate the finite element mesh. This creates an input data file for the analysis code (this file is identical to that of the serial code).
- Carry out the domain decomposition and generate input data specific to each of the processors. This data contains all the appropriate mesh and analysis information as well as the communication information required by the processors.
- Perform the explicit dynamic analysis in parallel. Each processor will generate output data particular to that domain.
- Collect information from the various domain outputs and generate, via an interface program, a file that the post-processor can utilize.

Within this system the only difference between the serial and parallel versions of the software from the user point of view is that he/she needs to select the number of processors and the type of domain decomposition algorithm. The domains can be viewed and various alternatives explored before the analysis is actually run. Even this stage may be hidden from the user [16,17].

The use of standard coding and PVM communication tools ensures that the parallel code SIMPACT can run on a heterogeneous network of computers that may include PC's, workstations and/or shared memory machines.

4 EXAMPLES

4.1 Two cylinders impact problem

This example analyses the deformation of two cylindrical tubes impacting with each other at right angles. The initial radius of the cylinders is R=0.1 m, the initial length is $L = 0.46$ m and the thickness is $t = 3$ mm. Each cylinder was modelled with 300 3-node Basic Shell Triangle (BST) (a total of 600 BST elements and 990 nodes). An initial velocity of 30 m/s, was applied to all the nodes of both cylinders and directed towards the opposite cylinder.

The analysis uses 1848 timesteps with an approximate average time increment of 4.33 nanoseconds for a whole analysis time of 8 milliseconds. The program automatically calculates the timestepping. The contact is activated throughout the analysis, with 12 levels of extended searching using a non-symmetric treatment. This means that penetration is only checked for the nodes of the slave surfaces against the master ones. The total CPU time used by one processor in one simulation was 12 seconds.

The initial meshes and the deformed ones can be seen in Figure 2. Results on the horizontal displacements of point A agree with the ones published in the technical literature [20],[21], [22] and [23] (Figure 4). Different domain decomposition meshes were performed in this test, some are shown in Figure 3; Speed-up results shown in Figure 5 indicate that six is the optimal number of domains for this example.

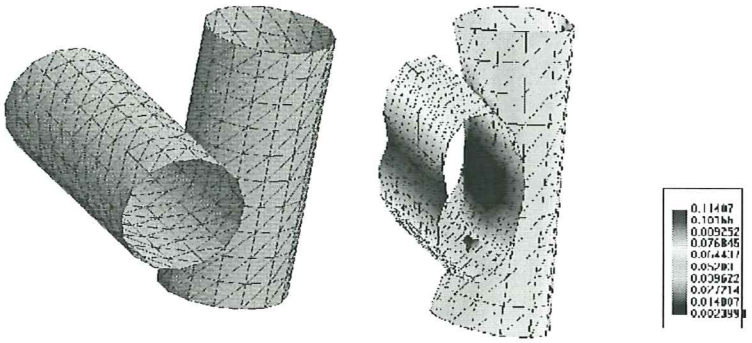

Figure 2. Two cylinders impact. Initial mesh and deformed mesh after impact

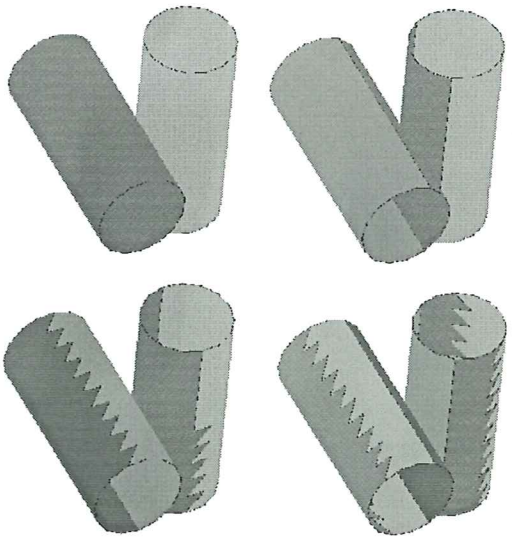

Figure 3. Cartesian domain decomposition in two, three, four and six domains

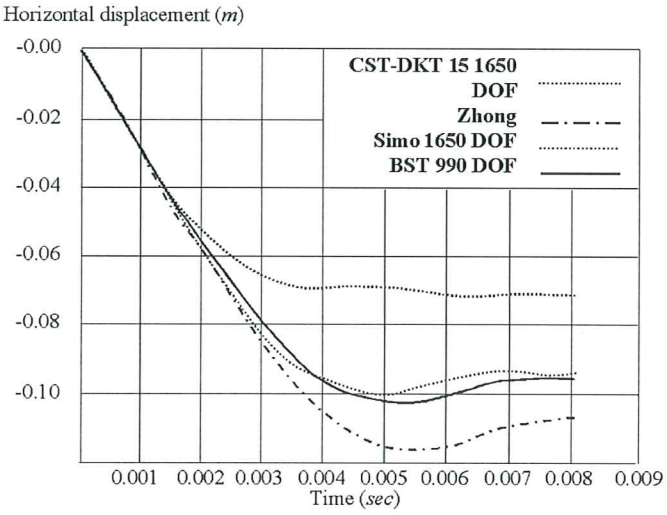

Figure 4. Analytical versus numerical results

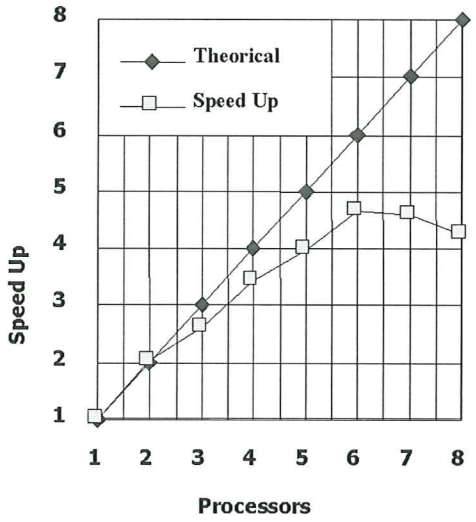

Figure 5. Speed-up for the two cylinders impact problem

4.2 Impact analysis of a baby car seat

The study presents a special interest in the automotive industry in order to design car seats. The loading consists of increasing and decreasing the acceleration applied to the structure between 0 and 28 g (g=10 m/s^2) in the zone where connection with the seat belts is assumed. The time interval to vary the acceleration is 0-70 ms, with a maximum value of 28 g corresponding to time 35 ms. A relaxation period of 50 ms was considered afterwards, when no acceleration is applied.

Figure 6 and presents the mesh in frontal and backside view of the analysed seat.

A mesh of 7360 BST elements and 64 beam elements was used. A dual PC (2 Processors PENTIUM II, 350 MHz configuration) was used to run the analysis based on a 2 domains decomposition procedure.

Figure 7 shows the evolution of the deformation state.

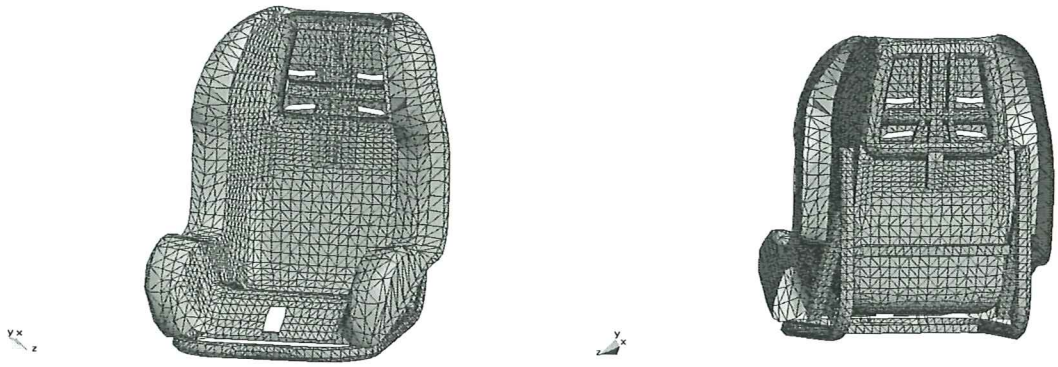

Figure 6. Frontal and backside view of the seat

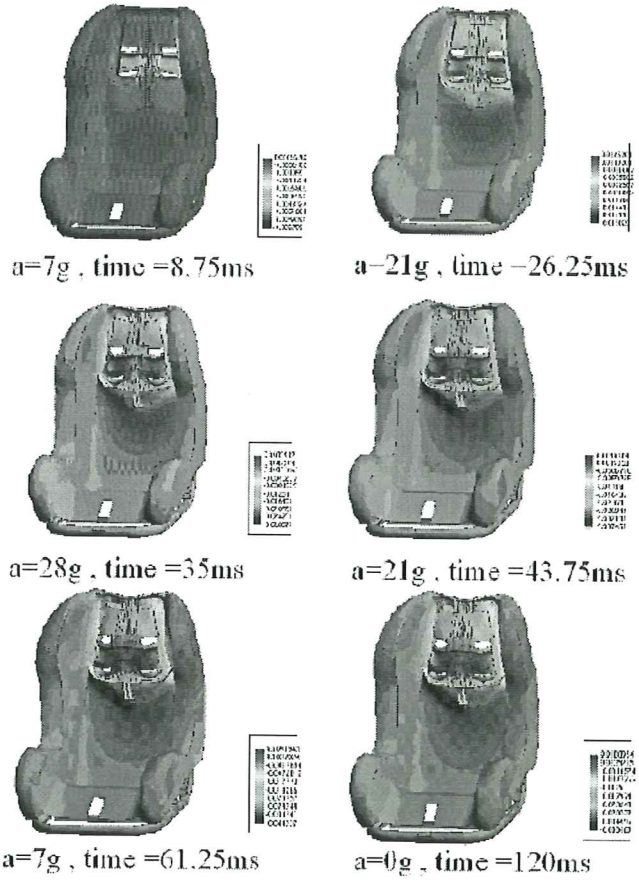

Figure 7. Evolution of the deformation state

4.3 Crash-worthiness analysis of a car under front impact

This example analyses a car structure in a frontal impact against a rigid wall. The simulation conditions are extracted from the Euro NCAP - the European New Car Assessment Programe - this implies an initial velocity of 17.8 m/s and also that the crash is across 40 per cent of the car's front.

The car structure was modelled by 110 000 BST elements and 60 000 nodes (mesh shown in Figure 8). Also 200 beam elements were introduced to modelize the joint motor-block and the lateral support beams. The contact is activated throughout the analysis, but without considering the self-contact betwen differents car structure parts.

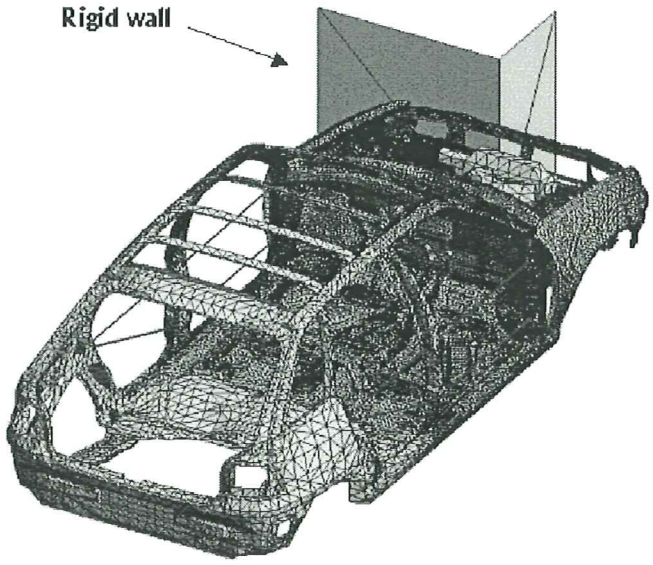

Figure 8. Car structure and rigid wall modelled

The analysis uses 44 088 time steps with an approximate average time increment of 0.75 microseconds for a whole analysis time of 30 miliseconds. The total CPU time used by two processors in one dual PC was 50 hours; it was used a parallel implementation (the two-domain decomposition is shown in Figure 9). The deformed mesh can be seen in Figure 10.

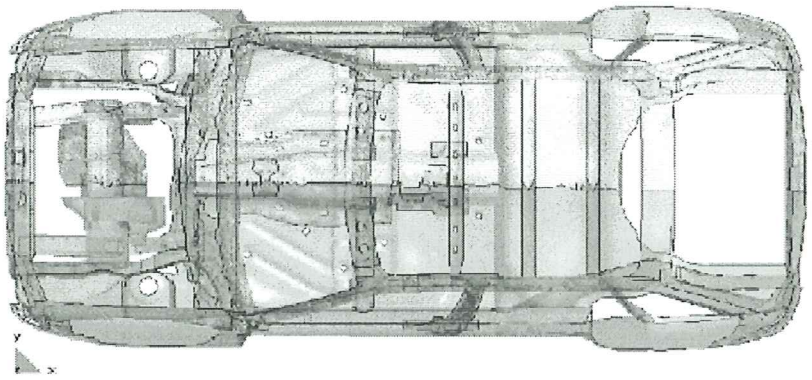

Figure 9. Car structure two domain decomposition

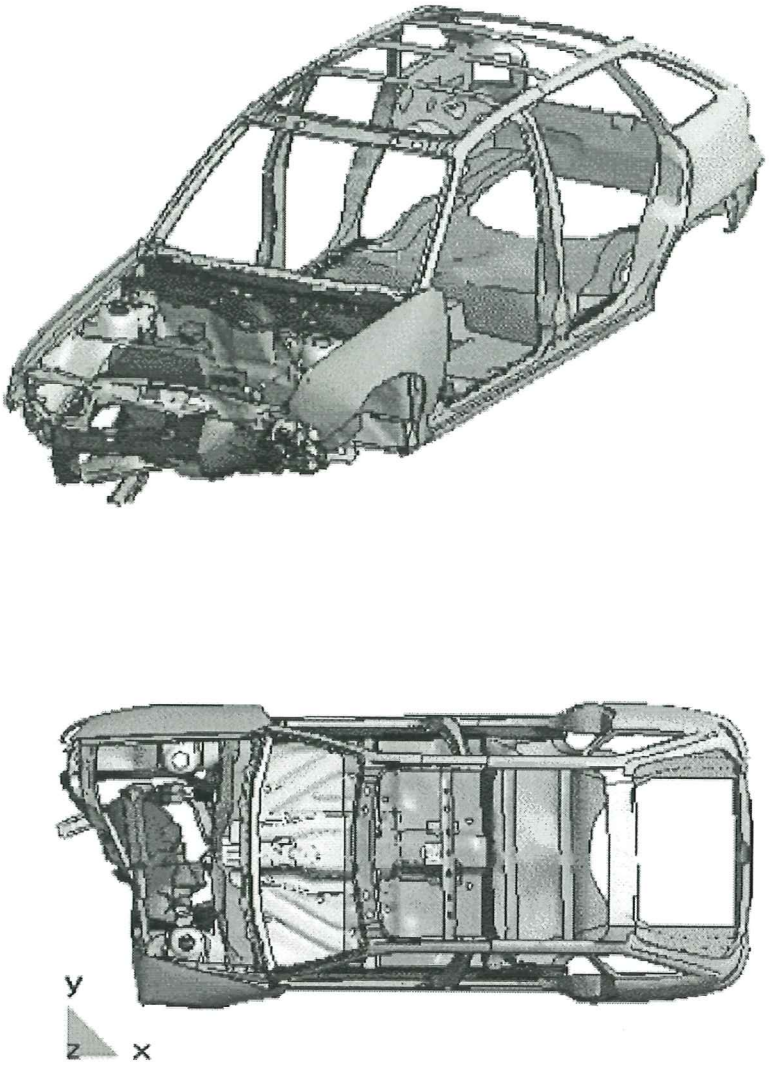

Figure 10. Deformation of the car structure after 30 ms following front impact

5 CONCLUDING REMARKS

The rotation free Basic Shell Triangle has proved to be an effective and accurate element for analysis of contact/impact problems of using an explicit dynamic approach. The simplicity of the element formulation favours its implementation into parallel computers in heterogeneous networks of PC's and workstations, thus allowing the solution of industrial crash-worthiness problems in competitive times.

REFERENCES

[1] Proceedings of IACM IV World Congress on Computational Mechanics, S. Idelsohn, E. Oñate and E.N. Dvorkin (Eds.), CIMNE, Barcelona, 1998.

[2] M.R. Barnes, "Form finding and analysis of tension space structure by dynamic relaxation", *Ph.D. Thesis*, Dept. of Civil Engineering, The City University, London, 1977.

[3] J.K. Hampshire, B.H.V. Topping and H.C. Chan, "Three node triangular elements with one degree of freedom per node", *Engng. Comput.* Vol. **9**, pp. 49–62, 1992.

[4] R. Phaal and C.R. Calladine, "A simple class of finite elements for plate and shell problems. I: Elements for beams and thin plates", *Int. J. Num. Meth. Engng.*, Vol. **35**, pp. 955–977, 1992.

[5] R. Phaal and C.R. Calladine, "A simple class of finite elements for plate and shell problems. II: An element for thin shells with only translational degrees of freedom", *Int. J. Num. Meth. Engng.*, Vol. **35**, pp. 979–996, 1992.

[6] D.Y. Yang, D.W. Jung, L.S. Song, D.J. Yoo and J.H. Lee, "Comparative investigation into implicit, explicit and iterative implic/explicit schemes for simulation of sheet metal forming processes" *NUMISHEET'93*, A. Makinouchi, E. Nakamachi, E. Oñate and R.H. Wagoner (Eds.), RIKEN, pp. 35–42, Tokyo, 1993.

[7] M. Brunet and F. Sabourin, "Prediction of necking and wrinkles with a simplified shell element in sheet forming", *Int. Conf. of Metal Forming Simulation in Industry*, Vol. II, pp. 27–48, B. Kröplin (Ed.), 1994.

[8] G. Rio, B. Tathi and H. Laurent, "A new efficient finite element model of shell with only three degrees of freedom per node. Applications to industrial deep drawing test", in *Recent Developments in Sheet Metal Forming Technoloy*, Ed. M.J.M. Barata Marques, 18th IDDRG Biennial Congress, Lisbon, 1994.

[9] E. Oñate and M. Cervera, "Derivation of thin plate bending elements with one degree of freedom per node", *Engng. Comput.* Vol. **10**, pp. 543–561, 1993.

[10] E. Oñate, M. Cervera and O.C. Zienkiewicz, "A finite volume format for structural mechanics", *Int. J. Num. Meth. Engng.*, **37**, pp. 181–201, 1994.

[11] S. Idelsohn and E. Oñate, "Finite volumes and finite elements: two 'good friends' *Int. J. Num. Meth. Engng.*, Vol. **37**, pp. 3323–3341, 1994.

[12] E. Oñate and F. Zárate, "New thin plate and shell triangles with translational degrees of freedom only", Presented at IUTAM/IACM Symposium, Viena, Austria, June 2-6, 1997.

[13] E. Oñate and F. Zárate, "Rotation free plate and shell triangles", Publication CIMNE no. 149, Barcelona 1999. To be published in *Int. J. Num. Meth. Engng.*

[14] E. Oñate, P. Cendoya, J. Rojek and J. Miquel, "A simple thin shell triangle with translational degrees of freedom for sheet stamping analysis", at *3rd International Conference on Numerical Simulation of 3D Sheet Forming Processes (NUMISHEET'96)*, Dearbon, Michigan, USA, 29 Sept. - 3 Oct., 1996.

[15] E. Oñate, P. Cendoya, J. Rojek and J. Miquel, "Non linear explicit dynamic analysis of shell structures using a simple triangle with translational degrees of freedom only", at the *Int. Conf. on Comput. Engng. Science (ICES'97)*, San Jose, Costa Rica, May 4–9, 1996.

[16] G.A. Duffett, L. Neamtu, E. Oñate, J. Rojek and F. Zárate, "Stampar: A parallel processing approach to sheet stamping simulations", in *Computational Plasticity V*, D.R.J. Owen, E. Oñate and E. Hinton (Eds.), CIMNE, Barcelona, 1997.

[17] SIMPACT. A finite element code for analysis of contact/impact problems, QUANTECH ATZ S.A., 1999.

[18] P. Cendoya, E. Oñate and J. Miquel, "Nuevos elementos finitos para el análisis dinámico elastoplástico no lineal de estructuras laminadas", (in Spanish), Monograph no. 36, CIMNE, Barcelona, 1997.

[19] O.C. Zienkiewicz and R.L. Taylor, "*The finite element method*", Mc.Graw Hill, 1989.

[20] O.Z.H. Zhong, "*Finite Element Procedures for Contact-Impact Problems*", Oxford University Press, U.K., 1993.

[21] J.L. Chenot, "A velocity approach to finite element calculation of elastoplastic and viscoplastic deformation processes", *Engng. Comput.*, Vol. **5**, pp. 2–9, 1988.

[22] J.C. Simo and D.D. Fox, "On stress resultant geometrically exact shell model. Part I: Formulation and optimal parametrization", *Comp. Meth. Appl. Mech. Engng.*, Vol. **72**, 267–304, 1989.

[23] J.C. Simo and D.D. Fox, "On stress resultant geometrically exact shell model. Part II: Computational Aspects of the non-linear theory", *Comp. Meth. Appl. Mech. Engng.*, Vol. **79**, 21–70, 1990.